Behavioral impulsivity is associated with pupillary alterations and hyperactivity in CDKL5 mutant mice

Aurelia Viglione[1,†], Giulia Sagona[2,†], Fabio Carrara[3], Giuseppe Amato[3], Valentino Totaro[1], Leonardo Lupori[2], Elena Putignano[4],

Tommaso Pizzorusso[1,4] and Raffaele Mazziotti [ID][2,*]

[1]BIO@SNS Lab, Scuola Normale Superiore, via Moruzzi 1, 56124 Pisa, Italy
[2]Department of Developmental Neuroscience, IRCCS Stella Maris Foundation, viale del Tirreno 331, 56128 Pisa, Italy
[3]ISTI—Istituto di Scienza e Tecnologia dell'Informazione, National Research Council, via Moruzzi 1, 56124 Pisa, Italy
[4]Institute of Neuroscience, National Research Council, via Moruzzi 1, 56124 Pisa, Italy
*To whom correspondence should be addressed at: Istituto Neuroscienze CNR, Via G. Moruzzi,1 56125 Pisa, Italy. Tel: +39 0503153167; Fax: +39 0503153220;
Email: raffaele.mazziotti@in.cnr.it

[†]These authors contributed equally to this work.

Abstract

Cyclin-dependent kinase-like 5 (*Cdkl5*) deficiency disorder (CDD) is a severe neurodevelopmental condition caused by mutations in the X-linked Cdkl5 gene. CDD is characterized by early-onset seizures in the first month of life, intellectual disability, motor and social impairment. No effective treatment is currently available and medical management is only symptomatic and supportive. Recently, mouse models of *Cdkl5* disorder have demonstrated that mice lacking *Cdkl5* exhibit autism-like phenotypes, hyperactivity and dysregulations of the arousal system, suggesting the possibility to use these features as translational biomarkers. In this study, we tested *Cdkl5* male and female mutant mice in an appetitive operant conditioning chamber to assess cognitive and motor abilities, and performed pupillometry to assess the integrity of the arousal system. Then, we evaluated the performance of artificial intelligence models to classify the genotype of the animals from the behavioral and physiological phenotype. The behavioral results show that CDD mice display impulsivity, together with low levels of cognitive flexibility and perseverative behaviors. We assessed arousal levels by simultaneously recording pupil size and locomotor activity. Pupillometry reveals in CDD mice a smaller pupil size and an impaired response to unexpected stimuli associated with hyperlocomotion, demonstrating a global defect in arousal modulation. Finally, machine learning reveals that both behavioral and pupillometry parameters can be considered good predictors of CDD. Since early diagnosis is essential to evaluate treatment outcomes and pupillary measures can be performed easily, we proposed the monitoring of pupil size as a promising biomarker for CDD.

Introduction

Mutations in cyclin-dependent kinase-like 5 (*Cdkl5*) cause *Cdkl5* deficiency disorder (CDD, *online mendelian inheritance in man* no. 300203). The disorder predominantly affects females heterozygous for mutations in *Cdkl5*, with an incidence of 1 per 42 000 live births (1). Hemizygous male cases have also been reported with a much lower prevalence (2,3). Mutations in the *Cdkl5* gene are currently one of the most common genetic causes of epilepsy in children (1). CDD has been genetically linked to multiple neurodevelopmental disorders, including Rett syndrome, early infantile epileptic encephalopathy and autism spectrum disorder [ASD; (4)]. However, today CDD is considered an autonomous etiopathological entity, with a clearly distinct genetic and clinical phenotype with respect to other similar infantile encephalopathies (5). *Cdkl5* encodes a serine/threonine kinase whose catalytic domains share homology with members of the cyclin-dependent kinase family and mitogen-activated protein kinases (6–8). In mice, *Cdkl5* is strongly upregulated postnatally and seems to be active both in the cytoplasm

and nucleus (9). *Cdkl5* was also found to be localized in postsynaptic structures, where it can regulate dendritic spine maturation and density, and regulate excitatory synaptic function (10,11). Recently has been shown that temporal manipulation of endogenous *Cdkl5* expression in adult mice can induce or rescue behavioral symptoms, demonstrating an indispensable role for *Cdkl5* also in the adult brain: postdevelopmental loss of *Cdkl5* disrupts many behavioral domains, hippocampal functional connectivity and dendritic spine morphology. In contrast, restoration of *Cdkl5* after the early stages of brain development using a conditional rescue mouse model, ameliorates CDD-related behavioral impairments and aberrant N-methyl-D-aspartate receptor signaling, suggesting the existence of a broad therapeutic time window for potential treatment (12). However, the role of *Cdkl5* in modulating neural substrates for cognitive and motor function is poorly understood and no effective treatment is currently available. Since 2012, multiple murine models of *Cdkl5* disorder have been generated, all of them showing similar behavioral deficits, highlighting the

reproducibility of CDD-related phenotypes in mice, and raising the possibility of preclinical testing of therapeutic strategies (4,13–15).

Recent studies have demonstrated that mice lacking *Cdkl5* exhibit impulsivity, and hyperlocomotion, resembling core symptoms of attention-deficit hyperactivity disorder [ADHD; (16–18)]. Deficits in attentional and executive functions in ADHD patients have been linked to dysregulations of arousal (19–21). The arousal system is a distributed network aimed to optimize the level of responsivity to sensory stimulation (22). The concept arises from classical electrophysiological studies relating to the different stages of sleep and wakefulness (23). Fluctuations in arousal are characterized by ultradian rhythmicity (24,25), they can also be elicited by external stimulation (26,27). The stimulus-evoked changes in arousal are generally referred to as orienting responses (28,29). The orienting response is an automatic and immediate response to an unexpected stimulus or changes in the environment (29–31) with effects on different levels of body responses [i.e. motor system, autonomic nervous system and central nervous system; (30–32)] including changes in pupil size and locomotion (33). Automatic orienting response to unexpected changes in the environment is a prerequisite for adaptive behavior; it is perceived as a disruption of the current attentional focus to immediately respond to changes in the environment on a physiological, behavioral and cognitive level (34). The arousal system is under the direct control of the noradrenergic circuit (along with acetylcholine) that widely innervates brain regions to control cortical processing (35,36), hippocampal excitability (37) and cognitive functions (37–39). Moreover, it controls many peripheral autonomous functions, like pupillary and cardiac levels, mediating complex behavioral outcomes, such as fight or flight response (40). Fluctuations in pupil size have been reported as a reliable index of arousal across species (41–47), including mice (48) and humans (49). Arousal alterations have also been documented in children with ASD and in a recent study revealed arousal alterations in *MeCP2*- and *Cdkl5*-deficient mouse models (40).

In order to evaluate psychomotor and cognitive abilities in *Cdkl5* mice, we performed an appetitive conditioning task in *Cdkl5* (P60) null mice ($Cdkl5^{-/y}$) and wild type (WT) littermates control ($Cdkl5^{+/y}$), using a 3D printed and automated appetitive operant conditioning chamber (50). Appetitive operant conditioning (51) is a standard technique used in experimental psychology in which animals, including rodents (52,53), learn to perform an action to achieve a reward. Using this paradigm makes it possible to extract learning curves, accurately measure mental chronometry (e.g. reaction times), and track an animal's position to assess motor and spatial performances (50). In addition, we performed pupillometry in *Cdkl5* male and female mutant mice and their WT littermates to assess the integrity of the arousal system by simultaneous

recording of pupil size and locomotor activity in basal conditions and in response to unexpected isoluminant stimuli presented in a virtual reality environment. The behavioral results indicated that CDD mice display an impulsive and hyperactive phenotype. Pupillometry showed decreased pupil size associated with hyperlocomotion and an impaired orienting response to virtual reality. Furthermore, we trained different machine learning models to recognize the genotype of the animals starting from behavioral and/or pupillometric data. This approach allows us to quantify the performances of the models to blindly classify subjects at a single animal level and evaluate analytically the quality of the biomarkers (54). These data reveal a global defect in arousal modulation in CDD mice and introduce metrics for quantitative, non-invasive and translational biomarkers for neurodevelopmental disorders.

Results

Abnormal behavior of male and female *Cdkl5* mutant mice in an automated appetitive operant conditioning task

During the operant conditioning task, the animal used its position to trigger a new trial by remaining in a specific place (active area, Fig. 1A) for a given amount of time (1.5 s). The visual stimulus consists of two bright blue dots, appearing above each response button. The mouse needs to touch one of the two buttons to obtain the reward (Fig. 1B). We found that $Cdkl5^{-/y}$ mice produced an increasingly higher number of trials than $Cdkl5^{+/y}$ mice, reaching a statistical difference on Day 3 (Fig. 1C). $Cdkl5^{-/y}$ mice also showed reduced reaction times (Fig. 1D) but no difference in intertrial intervals (time elapsing between the response and the activation of a novel trial, Fig. 1E). Moreover, the tracking analysis revealed altered locomotor activity in $Cdkl5^{-/y}$ mice. In particular, during the task, $Cdkl5^{-/y}$ mice moved faster and covered a greater distance than $Cdkl5^{+/y}$ (Supplementary Material, Fig. S1A–C).

Most CDD patients are heterozygous females carrying missense, nonsense, splice or frameshift *Cdkl5* gene mutations or a genomic deletion (55). In females, the phenotypic spectrum of the disease spans from mild to severe forms, whereas boys carrying mutations in *Cdkl5* have more severe epileptic encephalopathy than girls (56,57). Thus, we decided to test *Cdkl5* heterozygous female mice ($Cdkl5^{+/-}$). Again, we found that $Cdkl5^{+/-}$ mice performed a higher number of trials than control littermates ($Cdkl5^{+/+}$; Fig. 1F). In particular, we found a statistical difference in the number of trials performed, already present on Days 1 and 2 (Fig. 1F). $Cdkl5^{+/-}$ mice also showed reduced reaction times (Fig. 1G) and intertrial intervals compared with $Cdkl5^{+/+}$ (Fig. 1H). The tracking analysis revealed an enhanced locomotor activity in $Cdkl5^{+/-}$ mice, in terms of speed and distance traveled (Supplementary Material, Fig. S1D–F). Thus, $Cdkl5^{+/-}$ mice are also altered in this behavioral task.
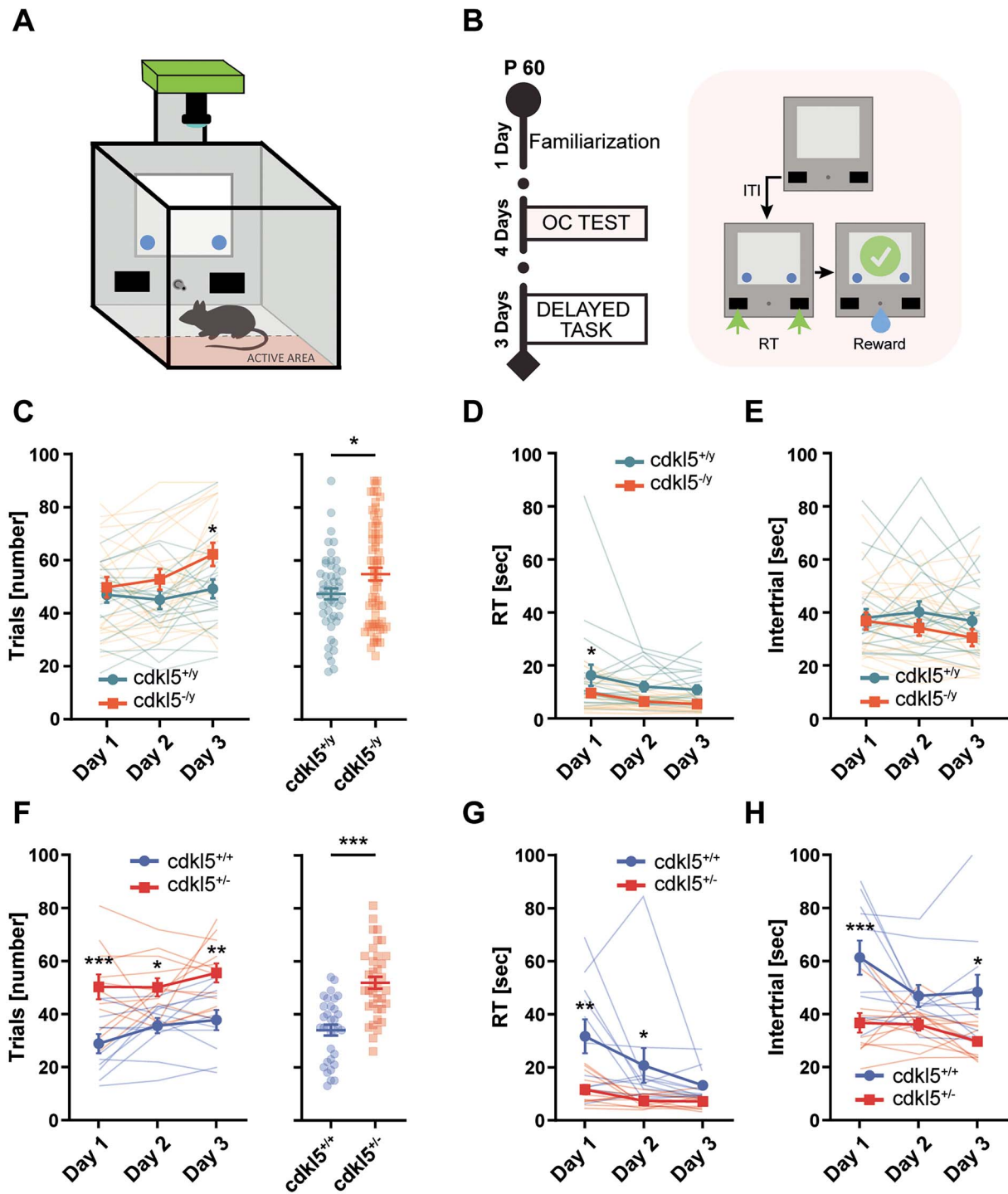
Figure 1. Appetitive operant conditioning test results in *Cdkl5* male and female mice. (**A**) Schematic representation of the conditioning chamber. (**B**) Diagram showing the appetitive conditioning timeline and paradigm. (**C**) On the left, single day trials in male mice: two-way analysis of variance (ANOVA), effect of time < 0.05, effect of genotype < 0.05; post hoc Sidak multiple comparisons at Day 3 < 0.05. On the right, cumulative number of trials performed in the 3 days of appetitive operant conditioning test: *P*-value < 0.05, unpaired *T*-test. (**D**) Reaction time in male mice: two-way ANOVA, effect of time < 0.005, effect of genotype < 0.005; post hoc Sidak multiple comparisons at Day 1 < 0.05. (**E**) Intertrial intervals in male mice show no differences between genotypes. (**F**) On the left, single day trials in female mice: two-way ANOVA, effect of genotype < 0.001; post hoc Sidak multiple comparisons at Day 1 < 0.001, Day 2 < 0.05 and Day 3 < 0.01. On the right, number of trials performed in the 3 days of shaping: *P*-value < 0.0001, unpaired *T*-test. (**G**) Reaction time in female mice: two-way ANOVA, effect of time < 0.05, effect of genotype < 0.05; post hoc Sidak multiple comparisons at Day 1 < 0.01, Day 2 < 0.05. (**H**) Intertrial intervals in female mice: two-way ANOVA, effect of time < 0.05, effect of genotype < 0.01; post hoc Sidak multiple comparisons at Day 1 < 0.001, Day 3 < 0.05. $n = 20$ *Cdkl5*$^{+/y}$; $n = 22$ *Cdkl5*$^{-/y}$; $n = 11$ *Cdkl5*$^{+/+}$; $n = 12$ *Cdkl5*$^{+/-}$. *P*-value < 0.05, **P*-value < 0.01 and ***P*-value < 0.001. OC: operant conditioning; RT: reaction time; ITI: intertrial.

Low level of cognitive flexibility, perseverative behavior and hyperactivity in *Cdkl5* null mice

To better investigate the hyperactive behavior observed in $Cdkl5^{-/y}$ mice, we introduced a modified version of the operant conditioning task: the delayed task (Fig. 2A). This test version increased the time needed to activate a single trial from 1.5 to 4 s, thus requiring a stronger inhibitory control. The delayed task revealed opposite results compared with the previous test: $Cdkl5^{-/y}$ mice performed a lower average number of trials than $Cdkl5^{+/y}$ littermates (Fig. 2B and C). In particular, we found a difference between groups in the number of trials performed on the first and second day of the delayed task (Post days 1 and 2). This difference disappears on the last day of the test when $Cdkl5^{-/y}$ mice reach the same performance as $Cdkl5^{+/y}$ mice (Fig. 2B, Post day 3). We did not find differences in the reaction times, demonstrating that the reduction in the number of trials was not attributable to a lack of interest in the task (Fig. 2D). However, we found a significant difference in the intertrial intervals. In particular, $Cdkl5^{-/y}$ mice showed longer intertrial intervals in the first 2 days of the delayed task (Fig. 2E). The diminished number of trials and longer intertrial intervals were caused by the higher number of invalid trials performed by Cdkl5$^{-/y}$ with respect to Cdkl5$^{+/y}$ mice. These findings demonstrate lower cognitive flexibility of $Cdkl5^{-/y}$ mice, probably because of an impairment in inhibitory control. We also introduced a new parameter called perseveration index to determine whether the learning impairment observed in $Cdkl5^{-/y}$ mice was associated with perseverative and impulsive behaviors. In detail, the perseveration index counts every time the mouse follows the previous rule instead of the new one (e.g. waiting for 1.5 s instead of 4 s in the active area). We found a significantly higher perseveration index in $Cdkl5^{-/y}$ mice compared with $Cdkl5^{+/y}$ on Post days 1 and 2 (Fig. 2F). This suggests that for the first 2 days of the delayed task, $Cdkl5^{-/y}$ mice continued to adopt the old operant task rules instead of adapting to the new paradigm, demonstrating an impairment in cognitive flexibility accompanied by impulsive and perseverative behaviors.

Head-fixed male and female *Cdkl5* mutant mice show an enhanced locomotor activity and a smaller pupil size

Pupil function abnormalities have been described in children with attention deficits (e.g. ADHD) and ASD (58,59). We performed pupillometry in P90 $Cdkl5^{-/y}$ mice and $Cdkl5^{+/y}$ littermates control (Fig. 3A). During pupillometry, mice were head-fixed and free to run on a circular treadmill equipped with an optical sensor to assess locomotor activity (Fig. 3B). Pupillometry was performed using the MEYE Deep Learning tool (47). During pupillometry, the animal was exposed to the following stimuli: a mean luminance uniform gray screen, a virtual reality isoluminant stimulus composed of a virtual corridor moving coherently with the animal movement to elicit

an orienting response and a high luminance white screen to assess the pupillary light reflex (Fig. 3B). The uniform gray background was also presented before and after orienting response and pupillary light reflex assessment to allow the pupil to return to baseline (Fig. 3B).

We first investigated pupil dynamics and locomotion in the absence of stimulation during the exposure to the uniform gray field. We found that $Cdkl5^{-/y}$ mice exhibit enhanced locomotor activity (Fig. 3C and D) also in the head-fixed condition. In particular, $Cdkl5^{-/y}$ mice showed more moving epochs and a higher velocity *per* epoch (Fig. 3D) than controls. We also found that the duration of a single running event was significantly longer in $Cdkl5^{-/y}$ mice compared with $Cdkl5^{+/y}$ (Fig. 3D). These results confirm in $Cdkl5^{-/y}$ mice the hyperactive phenotype observed in the appetitive operant conditioning chamber, suggesting the presence of altered arousal levels. Pupillometric analysis revealed a constitutively smaller pupil size in $Cdkl5^{-/y}$ mice compared with controls (Fig. 3E). However, the normalized pupil dilation present during running was unaffected (Supplementary Material, Fig. S2).

Locomotor activity and pupil size were also affected in $Cdkl5^{+/-}$ heterozygous female mice. In particular, locomotor activity was enhanced in $Cdkl5^{+/-}$ mice as compared with control female $Cdkl5^{+/+}$, both in terms of time spent running and velocity (Fig. 3F and G). Moreover, as in male mutants, $Cdkl5^{+/-}$ mice displayed a significantly smaller pupil size during the running state and a strong trend ($P = 0.057$) when resting (Fig. 3H).

Cdkl5 null mice show altered orienting response but intact pupillary light response

Previous studies have demonstrated atypical visuospatial orienting response in children with attention-related deficits and ASD (58,60,61). Thus, we investigated the orienting response induced by the virtual reality stimulus. $Cdkl5^{+/y}$ mice clearly showed an orienting response consisting of a substantial pupil dilation immediately after the stimulus onset. In contrast, $Cdkl5^{-/y}$ mice displayed a dramatically reduced and transient pupillary response (Fig. 4A). Virtual reality also induced different locomotor responses. In particular, although virtual reality elicited an increase in motility of $Cdkl5^{+/y}$ mice, $Cdkl5^{-/y}$ mice did not show significant changes in running velocity (Fig. 4B).

Finally, we tested whether the pupillary light reflex, an autonomic reflex that constricts the pupil in response to an increase in luminance, was changed in *Cdkl5* mutants. As shown in Figure 4C, we did not observe any significant differences in pupil constriction amplitude (maximal relative change in pupil area during constriction) or pupil re-dilation (maximal relative change in pupil area to recover the constriction, Fig. 4D). These results reveal an unaltered pupillary light reflex, suggesting a central origin for the orienting response alterations observed. Taken together, these results demonstrate in $Cdkl5^{-/y}$ mice an altered physiological and behavioral response to an orienting visual stimulus.
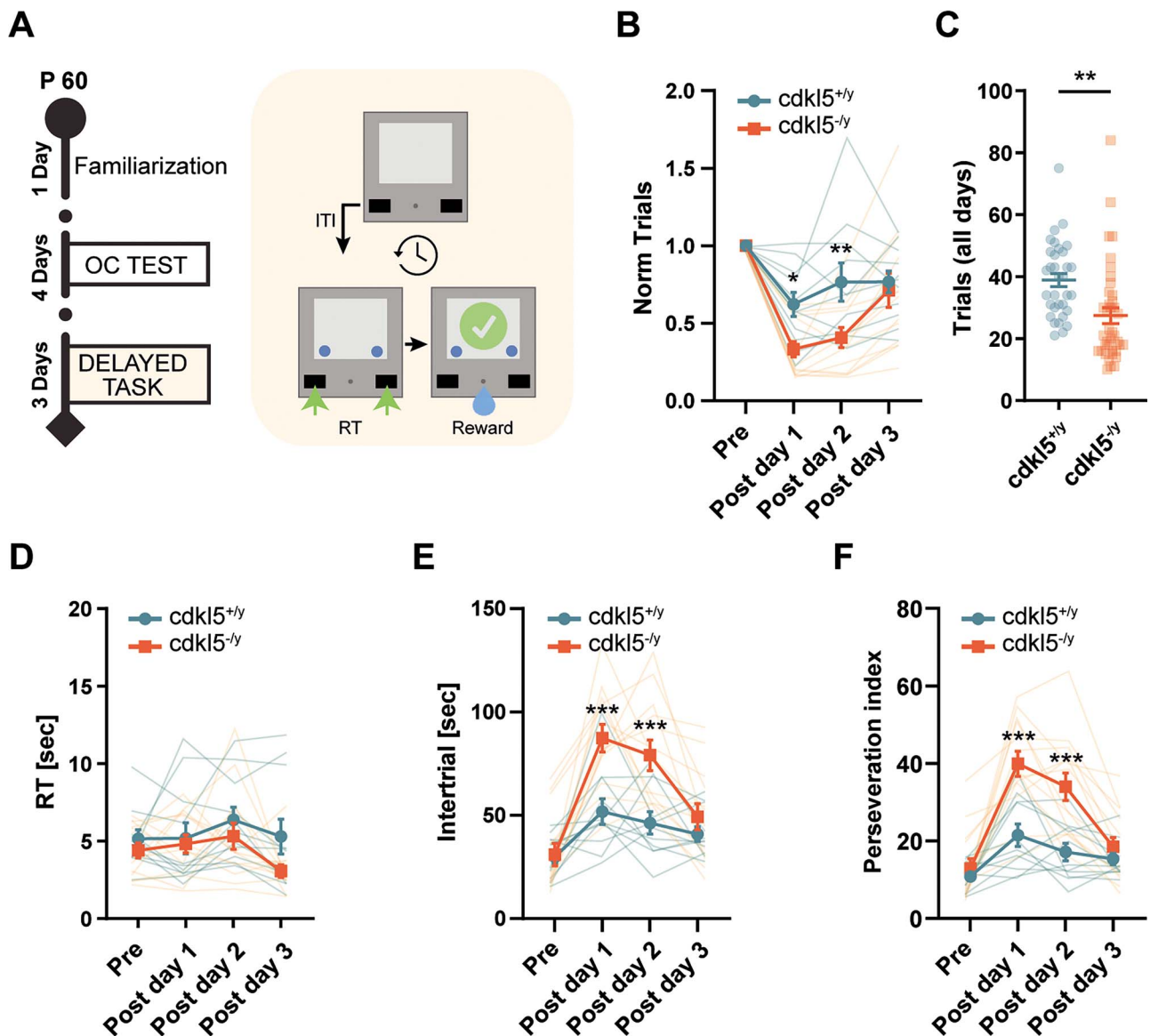
Figure 2. Delayed task in *Cdkl5* null mice. (**A**) Diagram showing the appetitive conditioning timeline and the delayed task paradigm. (**B**) Number of trials normalized on the last day of the appetitive operant conditioning test (Pre): two-way ANOVA, interaction time · genotype < 0.01, post hoc Sidak multiple comparisons at Day 5 < 0.05 and Day 6 < 0.01. (**C**) Number of trials performed in all the 3 days of delayed time: *P*-value < 0.01, unpaired *T*-test. (**D**) Reaction times show no differences between genotypes. (**E**) Intertrial intervals: two-way ANOVA, interaction time · genotype < 0.01, post hoc Sidak multiple comparisons at Post day 1 < 0.001 and Post day 2 < 0.001. (**F**) Perseveration index: two-way ANOVA, interaction time · genotype < 0.001, post hoc Sidak multiple comparisons at Post day 1 < 0.0001 and Post day 2 = 0.0001. $n = 11$ *Cdkl5*$^{+/y}$; $n = 13$ *Cdkl5*$^{-/y}$. *P-value < 0.05, **P-value < 0.01 and ***P-value < 0.001. OC: operant conditioning; RT: reaction time; ITI: intertrial.

Behavioral appetitive conditioning parameters and head-fixed pupillometric and behavioral responses are robust predictors of *Cdkl5* null mice alterations

To test whether the behavioral and pupillary alterations observed in *Cdkl5* null mice can be used to classify single animals, we employed machine learning algorithms to build models capable of predicting mouse genotype from the behavioral and pupillary alterations that we measured. We found that by training the models only with the behavioral parameters collected during the appetitive operant conditioning task, almost all the models showed a remarkable discriminative capability between mutated and WT mice. In particular, depending on the

model adopted, single mouse accuracy ranged between 77 and 83% and sensitivity between 75 and 87% (Table 1). The same machine learning models were employed to test the predictive power of the alterations found in *Cdkl5* mutant mice during pupillometry. Interestingly, we found that the pupillary and behavioral responses collected during the pupillometric assessments were good genotype predictors, with accuracy between 77 and 83% and sensitivity between 79 and 83% (Table 2). Finally, when we combined the models of the appetitive operant conditioning parameters with the parameters acquired during pupillometry, we found that the prediction power remarkably increased, reaching an accuracy between 77 and 91% and sensitivity between 73 and 91% (Table 3).
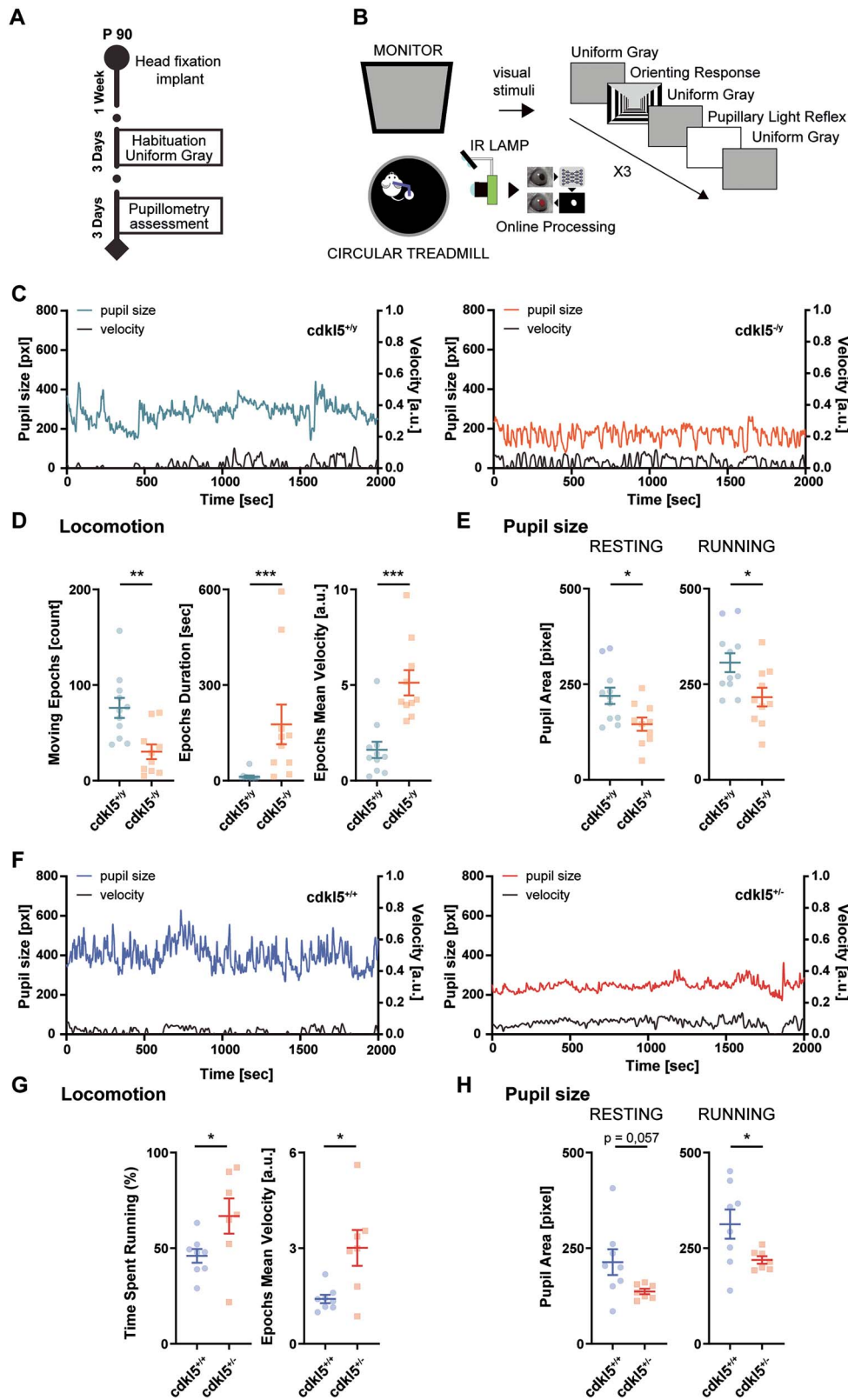
Figure 3. Locomotor activity and pupil size reveal arousal alterations in *Cdkl5* male and female mutant mice. (**A**) Diagram showing the pupillometry timeline. (**B**) Schematic representation of the head-fixed pupillometry setup. The mouse was head-fixed to a custom-made metal arm equipped with a 3D printed circular treadmill to monitor running behavior. In the meantime, we assessed: baseline pupil size (uniform gray screen), orienting response (to isoluminant virtual reality) and the pupillary light reflex (high luminance white screen). Each condition is repeated three times. We repeated the same protocol on three different days. (**C**) Pupil diameter trace from a WT male mouse (*Cdkl5*$^{-/y}$) and a *Cdkl5* null male mouse (*Cdkl5*$^{+/y}$). (**D**) *Cdkl5* null mice showed alterations in locomotor activity compared to WT: a decreased number of moving epochs (defined as a period of continuous movement): *P*-value < 0.01, unpaired *T*-test; an increase in the average duration of moving epoch: *P*-value < 0.05, unpaired *T*-test; and an increase in epochs mean velocity: *P*-value < 0.001, unpaired *T*-test. (**E**) *Cdkl5*$^{-/y}$ showed a constitutively smaller pupil size compared to *Cdkl5*$^{+/y}$ both during resting and running (resting,

Table 1. Genotype classification of machine learning models using operant conditioning parameters

Model	Accuracy (mean %)	Specificity (mean %)	Sensitivity (mean %)	Permutation scores (%)	P-value	Significance
SVC	82.8	88.4	78.6	52.5	< 0.01	**
MLP classifier	82.5	80.0	86.8	53.1	< 0.01	**
Gaussian process classifier	81.9	85.2	83.2	52.8	< 0.01	**
Decision tree classifier	81.3	84.3	81.0	51.0	< 0.01	**
AdaBoost classifier	81.2	83.9	83.0	51.6	0.02	*
Logistic regression	76.9	80.3	75.25	53.3	< 0.01	**
K neighbors classifier	74.2	84.8	66.3	52.9	0.12	ns
Dummy classifier	50.4	51.2	48.4	50.1	0.47	ns

Abbreviations: OC, operant conditioning; ns, not significant.

Table 2. Genotype classification of machine learning models using head-fixed condition parameters

Model	Accuracy (mean %)	Specificity (mean %)	Sensitivity (mean %)	Permutation scores (%)	P-value	Significance
Logistic regression	83.1	86.1	82.5	52.3	0.02	*
MLP classifier	81.7	82.9	83.1	51.2	0.02	*
SVC	81.0	82.2	80.9	49.9	<0.01	**
AdaBoost classifier	80.1	87.7	74.3	50.0	0.02	*
Decision tree classifier	79.7	85.7	73.1	50.3	<0.01	**
Gaussian process classifier	77.1	79.4	79.7	50.4	0.02	*
K neighbors classifier	73.7	74.8	74.7	49.2	0.11	ns
Dummy classifier	48.8	47.3	49.9	50.6	0.18	ns

Abbreviations: OR, orienting response; ns, not significant.

Discussion

This study reports alterations in behavioral and physiological parameters of male *Cdkl5* deficient and female heterozygous mice capable of classifying CDD subjects with high accuracy and sensitivity. Behavioral impairment was assessed in an appetitive operant conditioning task using a fully automated and standardized appetitive operant conditioning chamber (50). In agreement with previous studies (16–18), the appetitive operant conditioning task revealed hyperactive and impulsive behavior in both male and female *Cdkl5* mutant mice. Intriguingly, differences in the strategies employed of mutant female and male mice appeared. Indeed, female mutants showed a difference already during the first day of testing. Although this difference could be further explored, it could be related to the sex influence on the strategies used during reinforcement learning displayed by mice. Indeed, previous studies showed that WT female mice had faster task acquisition than males. Thus, a deficit present in CDKL5 deficient mice could emerge at earlier time points than in males (62). We also demonstrated lower levels of cognitive flexibility, linked to an impairment in inhibitory control in *Cdkl5* null mice. Indeed, although mutant mice could successfully perform more trials than controls if they had to wait only for a short time, they persevered with the previous strategy if the waiting time was prolonged, resulting in less successful

trials than controls. This deficit is transient, returning to WT levels in 3 days and suggesting the presence of slower residual flexibility in *Cdkl5* null mice. Inhibitory control, such as cognitive flexibility, is an executive function mediated by the prefrontal cortex (63), which implies being able to control impulses, and old habits of thought or action [e.g. conditioned responses; (64)]. Impairments in executive abilities such as cognitive flexibility and inhibitory control have been identified in individuals with ASD (65). In particular, deficits in inhibitory control were associated with restricted and repetitive behaviors (66). Intriguingly, symptoms of inattention and hyperactivity, typical features of ADHD, have been frequently documented in children with ASD (67) and could also be present in CDD patients, although the *Cdkl5* gene has not been linked to ADHD in a genome-wide association study (68). Previous studies showed that impulsivity and hyperlocomotion of *Cdkl5* null mice could be corrected by methylphenidate, an inhibitor of the dopamine transporter clinically effective in improving ADHD symptoms, suggesting a role for dopaminergic impairment in mediating impulsivity deficits (16,17).

Arousal impairment in *Cdkl5* null and heterozygous mice

Our study shows that the presence of hyperactivity is also associated with impairment in processes controlling

P-value < 0.05; running, P-value < 0.05; unpaired T-test). (**F**) Pupil diameter trace from a WT female mouse (*Cdkl5*$^{+/+}$) and a *Cdkl5* heterozygous female mouse (*Cdkl5*$^{+/-}$). (**G**) *Cdkl5*$^{+/-}$ mice showed an enhanced locomotor activity compared to *Cdkl5*$^{+/+}$, in terms of percentage of time spent running, P-value < 0.05, unpaired T-test and velocity, P-value < 0.05, unpaired T-test. (**H**) *Cdkl5*$^{+/-}$ mice showed a baseline smaller pupil size compared to *Cdkl5*$^{+/+}$ during running, P-value < 0.05, unpaired T-test, and a strong trend in resting, P-value = 0.057, unpaired T-test. $n = 11$ *Cdkl5*$^{+/y}$, $n = 10$ *Cdkl5*$^{-/y}$; $n = 8$ *Cdkl5*$^{+/+}$, $n = 7$ *Cdkl5*$^{+/-}$. *P-value < 0.05, **P-value < 0.01 and ***P-value < 0.001.

Table 3. Genotype classification of machine learning models using operant conditioning and head-fixed parameters

Model	Accuracy (mean %)	Specificity (mean %)	Sensitivity (mean %)	Permutation scores (%)	P-value	Significance
MLP classifier	91.4	92.6	91.7	51.1	0.02	*
Logistic regression	88.8	89.6	88.3	50.8	0.04	*
SVC	87.7	92.9	84.4	50.6	< 0.01	**
Gaussian process classifier	86.6	93.6	81.0	50.4	< 0.01	**
K neighbors classifier	82.4	94.5	70.5	51.2	< 0.01	**
Decision tree classifier	78.8	86.1	72.6	50.8	< 0.01	**
AdaBoost classifier	77.2	82.8	73.7	51.2	< 0.01	**
Dummy classifier	51.5	50.8	52.5	49.2	0.62	ns

Abbreviations: OC, operant conditioning; OR, orienting response; ns, not significant.

general arousal in *Cdkl5* mice assessed by measuring pupil size regulation and locomotor behavior. We found that *Cdkl5* mutants stay longer than wild-type mice in a high arousal state characterized by a dilated pupil and running. Absolute values of pupil size were always significantly smaller than controls in both male null and female heterozygous *Cdkl5* mutant mice, although relative pupillary dilation during running or pupillary response to illumination change was unaffected. Constitutive smaller pupil size is reported to be linked with working memory and cognitive abilities and could be related to altered activity of the locus coeruleus-noradrenergic system (69–71). Our study also revealed alterations in pupillary response to unexpected visual stimuli, a component of the orienting response commonly used also for human assessment (33). Indeed, we found that wild-type mice exhibited a considerable and sustained pupil dilation in response to unexpected stimuli, whereas mutants showed a smaller and transient dilation. The presentation of the unexpected stimulus also led to an increased running in wild-type mice but not in mutant mice.

Previous studies showed that cortical processing of visual stimuli is altered in mice carrying mutations of the CDKL5 gene (54). This comprises aberrant visual cortical responses, and moderately reduced contrast sensitivity and visual acuity. Aware of this limitation, we designed the virtual reality environment, adopted as orienting stimulus, with a spatial frequencies content (0.06–0.1 cyc/deg) and contrast (90%), well within the visual perceptual thresholds of mutants mice. However, arousal alterations per se could affect perception since an interaction between arousal (and behavioral state) and visual (in general sensory) perception has been clearly revealed by studies on the visual primary areas both in mice (72,73) and in humans (74,75). Further studies on the interaction between arousal and visual perception in CDKL5 mutant mice could elucidate the presence of possible bidirectional effects.

Overall, these data are consistent with a scenario in which *Cdkl5* mutants are most of the time in a high arousal state that is not further increased by novel stimuli. Notably, the pupillary light reflex analysis did not show alterations, demonstrating that the observed pupillary alterations are attributable to central dysfunctions rather than iris muscle or autonomic control abnormalities. The central origin of these deficits is in line with a recent study by Artoni *et al.* (40) revealing broadly distributed pupil sizes as a signature shared by mouse models of idiopathic or monogenic ASD, comprising CDD. In particular, in this study, the pupillary deficit of MeCP2 deficient mice could be rescued by the selective expression of MeCP2 in cholinergic circuits. The combination of behavioral inflexibility and arousal deficits could arise from alterations in the multistage neural pathways between the prefrontal cortex and subcortical nuclei, such as the striatum and the subthalamic nucleus that have been proposed to support inhibitory control and behavioral states through direct and indirect routes (76,77). *Cdkl5* mRNA is expressed in cholinergic nuclei and superior colliculus (mousebrain.org), two structures implicated in central pupillary control and orienting response (33,78). However, an indepth investigation is needed to clarify this point.

Machine learning reveals a robust biomarker of CDD

Our machine learning models revealed that behavioral impulsivity and orienting response assessed by pupillometry are good predictors of CDD, with an enhanced power when evaluated together. Pupillometry is a non-invasive, quantitative and fully translational tool already used in clinical practice that requires minimal collaboration by the subject, and it has been used even in newborns and preterm infants at postpartum age of 1 day (79). Recently developed methods are opening the possibility to perform these measurements in a clinical and a domestic environment (47). Since early diagnosis is essential to evaluate treatment outcomes and pupillary measures can be performed quickly, also in preverbal subjects, we propose the monitoring of resting-state and orienting response pupillometry as a promising and practical biomarker for CDD. The presence of arousal impairments in different neuropsychiatric disorders raises the possibility that pupillometry could be used also in ASD (80) and ADHD (81) or in psychiatric conditions involving arousal alterations such as bipolar disorder.
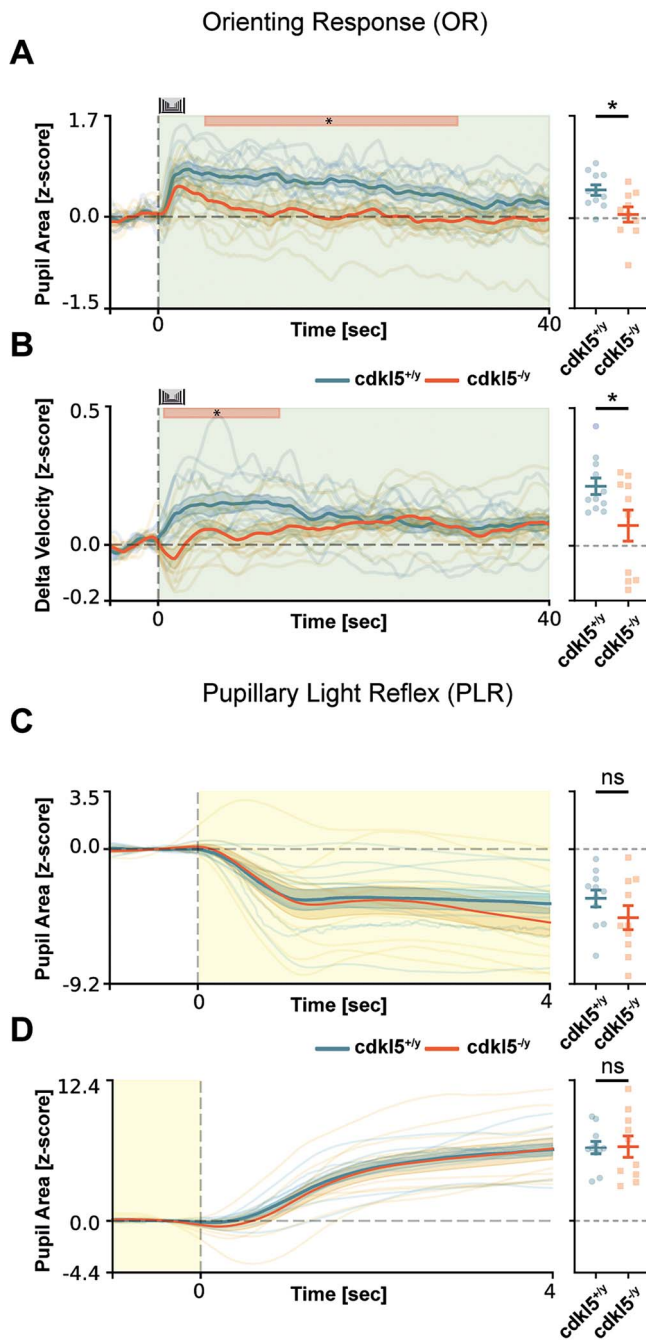
Figure 4. Pupillary orienting response and pupillary light reflex assessment. (**A**) On the left, the average fluctuation of pupil size for all the stimulus repetitions. On the right the average pupil size. During the presentation of the orienting stimulus, $Cdkl5^{-/y}$ mice showed a reduced pupillary dilation compared to $Cdkl5^{+/y}$ (P-value < 0.05, unpaired T-test); the shaded area represents the presentation of the virtual reality (VR) stimulus. (**B**) On the left, the average running velocity for all the stimulus repetitions. On the right the average velocity. $Cdkl5^{y-/y}$ mice showed a different behavioral response compared with $Cdkl5^{+/y}$ (P-value < 0.05, unpaired T-test), the shaded area represents the presentation of the VR stimulus. (**C, D**) PLR response reveals no significant differences in both pupil constriction (top) and pupil re-dilation (bottom) between $Cdkl5^{-/y}$ mice and $Cdkl5^{+/y}$. On the left, single animal traces and average fluctuation (thick line) of pupil size. Shaded area represents the presentation of the high luminance stimulus. Vertical dashed lines represent the onset of the visual stimulus. On the right the average pupil size during pupil constriction and pupil re-dilation. $n = 11$ $Cdkl5^{+/y}$, $n = 10$ $Cdkl5^{-/y}$. *P-value < 0.05, ns = not significant.

Materials and Methods
Animal handling
Animals were maintained in rooms at 22°C with a standard 12 h light–dark cycle. During the light phase, a constant illumination below 40 lux from fluorescent lamps was maintained. Food (standard diet, 4RF25 GLP Certificate, Mucedola) and water were available *ad libitum* and changed weekly. Open-top cages with wooden dust-free bedding were used. All the experiments were carried out according to the directives of the European Community Council (2011/63/EU) and approved by the Italian Ministry of Health. All necessary efforts were made to minimize both stress and the number of animals used. The mice used in this work derive from the *Cdkl5* null strain in C57BL/6N background developed in (13), and backcrossed in C57BL/6J for seven generations. Male WT mice were bred with female heterozygous to obtain mutant and WT littermates. Weaning was performed on postnatal day (P)21–23. Genotyping (P10–12) was performed on tail tissue as described in (13). We tested mice from P60 to P120. Colony founders were selected for the absence of the rd8 retinal degeneration allele spontaneously present in C57BL/6N mice (82). Data analyses were performed by experimenters blind to the genotype.

The appetitive operant conditioning protocol
To perform the appetitive conditioning task we used a custom-made appetitive operant conditioning chamber, as described in Mazziotti *et al.* (50). Before starting the experiments, mice were handled for 1 week 5 min per day. During appetitive operant conditioning protocol, mice were water restricted (all mice maintained a body weight above 85% of their baseline). We performed the first day of familiarization, by placing each animal in the appetitive operant conditioning box for three sessions of 10 min, spaced by at least 2 h between each other. During this phase, a liquid reward (1% saccharin), coupled with the reward tone (3300 Hz), is provided manually whenever the mouse is in the active area (located on the side opposite to the interface wall), in this way the animal learns where to find the reward and associate it with the tone. The day after the familiarization we start the OC task (3 sessions per day, duration: 4 days). In the OC phase a visual stimulus was introduced, consisting of two bright blue dots (luminance: 0.9 cd/m², wavelength: 465–475 nm, diameter: 5 mm) that appear above the two buttons after waiting for 1.5 s in the activation area. Mice must touch one of the two buttons to obtain the liquid reward. We quantify the number of trials per session, the reaction time (the time between the activation of the trial and the button touch), the intertrial interval (the time elapsed between the response and the activation of a new trial), the speed and distance traveled. The second group of mice, after the appetitive operant conditioning task, was introduced to the delayed task (duration 3 days). In this new version of the test, the time needed to activate a

new trial was extended from 1.5 to 4 s. In order to evaluate the ability to inhibit a learned automatic response, we also introduced the perseveration index using a custom-made Matlab software processing the mouse-tracking data. To analyze mouse-tracking data the arena is virtually divided into 256 (16 × 16) bins and raw exploration is z-scored to obtain relative exploration measures. In particular, a perseveration was counted every time the mouse exited the active zone before the 4 s limit.

Surgery

Mice were deeply anesthetized using isoflurane (3% induction and 1.5% maintenance), placed on a stereotaxic frame and head-fixed using ear bars. Prilocaine was used as a local anesthetic for the acoustic meatus. Body temperature was maintained at 37° using a heating pad, monitored by a rectal probe. The eyes were treated with a dexamethasone-based ophthalmic ointment (Tobradex, Alcon Novartis) to prevent cataract formation and keep the cornea moist. Respiration rate and response to toe pinch were checked periodically to maintain an optimal level of anesthesia. Subcutaneous injection of Lidocaine (2%) was performed prior to scalp removal. The Skull surface was carefully cleaned and dried, and a thin layer of cyanoacrylate was poured over the exposed skull to attach a custom-made head post that was composed of a 3D printed base equipped with a glued set screw (12 mm long, M4 thread, Thorlabs: SS4MS12). The implant was secured to the skull using cyanoacrylate and UltraViolet curing dental cement (Fill Dent, Bludental). At the end of the surgical procedure, the mice recovered in a heated cage. After 1 h, the mice were returned to their home cage. Paracetamol was used in the water as antalgic therapy for 3 days. We waited for 7 days before performing head-fixed pupillometry to provide sufficient time for the animals to recover.

Pupillometry

During pupillometry, mice were head-fixed and free to run on a circular treadmill. We employed a modified version of the apparatus proposed by Silasi *et al.* (83), equipped with a 3D printed circular treadmill (diameter: 18 cm). Velocity was detected using an optical mouse below the circular treadmill. To record the pupil, we used a universal serial bus camera (oCam-5CRO-U, Withrobot Lens: M12 25 mm) connected to a Jetson AGX Xavier Developer Kit (NVIDIA) running a custom Python3 script (30fps). Real-time pupillometry was performed using MEYE (47), a convolutional neural network that performs online pupillometry in mice and humans (47). Before the experiments, mice were handled for 1 week 5 min each day; then, they were introduced gradually to head-fixation for an increasing amount of time for 3 days (habituation). During days 1 and 2, we performed two sessions of 10 min of head-fixation, one in the morning and one in the afternoon. On Day 3, we performed one session of 20 min. During each head-fixation session, a curved monitor (24 inches Samsung, CF390) was placed

in front of the animal (at a distance of 13 cm), showing a uniform gray with a mean luminance of 8.5 cd/m^2. After the habituation phase, we performed the pupillary assessments. The assessment contains different epochs:

1. Uniform gray screen with a mean luminance (duration: 225 s, mean luminance: 8.5 cd/m^2). To allow the pupil to return to baseline, a uniform gray screen is also presented for 60 s between each stimulation.
2. VR coherent with the animal movement eliciting an orienting response (180 s). Composed of a luminance linearized procedural virtual corridor written in C# and running in Unity. The virtual corridor was composed of sine-wave gratings at different orientations (walls at 0° and floor at 90°) and spatial frequencies (from 0.06 to 0.1 cycles/deg), with a mean luminance of 8.5 cd/m^2. The animal position in the virtual corridor was updated using an optical mouse connected to the circular treadmill.
3. PLR (15 s white screen. Luminance: 30 cd/m^2).

Each epoch is presented three times for a total duration of 30 min.

For the pupillary assessment of female mice, we evaluated baseline pupil size and locomotion during the presentation of a uniform gray screen with a mean luminance of 8.5 cd/m^2.

Machine learning

Machine learning models were fitted and evaluated using Python and Scikit-Learn.

All adopted models are binary classifiers predicting the genotype from numeric behavioral and physiological features. We considered as behavioral parameters, the number of trials per session, the reaction time and the intertrial interval during the appetitive operant conditioning test and delayed task; as physiological features, we considered the average pupil size in resting and in running, the running speed, the running duration and the pupillary ratio between resting and running in the different visual presentations.

Input features are standardized before training. The specific models we adopt, together with the hyperparameter we tuned, are the following. The default Scikit-Learn parameters were used, if otherwise not specified.

A. Logistic regression with L2 regularization (84); regularization strength is searched in logarithmic scale in [10^{-4}, 10^5].
B. Support vector machine classifier [SVC, (85)]; we test linear and Gaussian kernels; the regularization parameter and the kernel scaling coefficient (only for Gaussian kernels) are searched in logarithmic scale respectively in [10^{-4}, 10^5] and [2^{-4}, 2^5].
C. Gaussian process classifier (86) with unitary RBF kernel.
D. Decision tree (87) with maximum depth searched in [1, 6].

E. AdaBoost classifier (88) with a 1-level-deep decision tree as a base estimator.

F. K-nearest neighbors classifier with uniform neighbors weighting; the best number of neighbors k is searched in [1,3].

G. Multi-layer perceptron (MLP) classifier (89) with one 100-neuron hidden layer and ReLU activation; the network is trained with the Adam optimizer for 1000 iterations; the learning rate and L2 regularization strength parameters are grid-searched respectively in [0.001, 0.01 and 0.1] and [0.0001, 0.01, 1 and 10].

For each model and each configuration of hyperparameters, the mean and standard deviation of accuracy, specificity and sensitivity are computed using 100 bootstrapped data splits; in addition, a permutation test with 100 permutations is performed using the 5-fold accuracy as a score. For brevity, only the best-performing configuration of hyperparameters is reported for each model. As a baseline, we also report the performance of the random classifier (dummy classifier).

Data analysis and statistics

Data analysis was performed using Python (Pupillometry and locomotion activity) and Matlab (Appetitive operant conditioning). Resting and running epochs are identified using an automated algorithm written in Python. The beginning of a moving epoch is defined as a period of at least 2 s in which velocity is higher than 1% with respect to the peak velocity of the subject. The epoch ends when velocity is below 1% for at least 2 s.

The statistical analysis was performed using Python custom scripts and GraphPad Prism 7.

Supplementary Material

Supplementary Material is available at *HMG* online.

Acknowledgements

Conflict of Interest statement. The authors declare that they have no competing interests.

Funding

References

1. Symonds, J.D., Zuberi, S.M., Stewart, K., McLellan, A., O'Regan, M., MacLeod, S., Jollands, A., Joss, S., Kirkpatrick, M., Brunklaus, A. *et al.* (2019) Incidence and phenotypes of childhood-onset genetic epilepsies: a prospective population-based national cohort. *Brain*, **142**, 2303–2318.

2. Olson, H.E., Demarest, S.T., Pestana-Knight, E.M., Swanson, L.C., Iqbal, S., Lal, D., Leonard, H., Cross, J.H., Devinsky, O. and Benke, T.A. (2019) Cyclin-dependent kinase-like 5 deficiency disorder: clinical review. *Pediatr. Neurol.*, **97**, 18–25.

3. Demarest, S.T., Olson, H.E., Moss, A., Pestana-Knight, E., Zhang, X., Parikh, S., Swanson, L.C., Riley, K.D., Bazin, G.A., Angione, K. *et al.* (2019) CDKL5 deficiency disorder: relationship between genotype, epilepsy, cortical visual impairment, and development. *Epilepsia*, **60**, 1733–1742.

4. Wang, I.-T.J., Allen, M., Goffin, D., Zhu, X., Fairless, A.H., Brodkin, E.S., Siegel, S.J., Marsh, E.D., Blendy, J.A. and Zhou, Z. (2012) Loss of CDKL5 disrupts kinome profile and event-related potentials leading to autistic-like phenotypes in mice. *Proc. Natl. Acad. Sci. U. S. A.*, **109**, 21516–21521.

5. Fehr, S., Wilson, M., Downs, J., Williams, S., Murgia, A., Sartori, S., Vecchi, M., Ho, G., Polli, R., Psoni, S. *et al.* (2013) The CDKL5 disorder is an independent clinical entity associated with early-onset encephalopathy. *Eur. J. Hum. Genet.*, **21**, 266–273.

6. Moseley, B.D., Dhamija, R., Wirrell, E.C. and Nickels, K.C. (2012) Historic, clinical, and prognostic features of epileptic encephalopathies caused by CDKL5 mutations. *Pediatr. Neurol.*, **46**, 101–105.

7. Weaving, L.S., Christodoulou, J., Williamson, S.L., Friend, K.L., McKenzie, O.L.D., Archer, H., Evans, J., Clarke, A., Pelka, G.J., Tam, P.P.L. *et al.* (2004) Mutations of CDKL5 cause a severe neurodevelopmental disorder with infantile spasms and mental retardation. *Am. J. Hum. Genet.*, **75**, 1079–1093.

8. Fuchs, C., Gennaccaro, L., Trazzi, S., Bastianini, S., Bettini, S., Lo Martire, V., Ren, E., Medici, G., Zoccoli, G., Rimondini, R. *et al.* (2018) Heterozygous CDKL5 knockout female mice are a valuable animal model for CDKL5 disorder. *Neural Plast.*, **2018**, 1–18.

9. Rusconi, L., Salvatoni, L., Giudici, L., Bertani, I., Kilstrup-Nielsen, C., Broccoli, V. and Landsberger, N. (2008) CDKL5 expression is modulated during neuronal development and its subcellular distribution is tightly regulated by the C-terminal tail. *J. Biol. Chem.*, **283**, 30101–30111.

10. Ricciardi, S., Ungaro, F., Hambrock, M., Rademacher, N., Stefanelli, G., Brambilla, D., Sessa, A., Magagnotti, C., Bachi, A., Giarda, E. *et al.* (2012) CDKL5 ensures excitatory synapse stability by reinforcing NGL-1–PSD95 interaction in the postsynaptic compartment and is impaired in patient iPSC-derived neurons. *Nat. Cell Biol.*, **14**, 911–923.

11. Della Sala, G., Putignano, E., Chelini, G., Melani, R., Calcagno, E., Michele Ratto, G., Amendola, E., Gross, C.T., Giustetto, M. and Pizzorusso, T. (2016) Dendritic spine instability in a mouse model of CDKL5 disorder is rescued by insulin-like growth factor 1. *Biol. Psychiatry*, **80**, 302–311.

12. Terzic, B., Felicia Davatolhagh, M., Ho, Y., Tang, S., Liu, Y.-T., Xia, Z., Cui, Y., Fuccillo, M.V. and Zhou, Z. (2021) Temporal manipulation of Cdkl5 reveals essential postdevelopmental functions and reversible CDKL5 deficiency disorder–related deficits. *J. Clin. Invest.*, **131**, 1–14.

13. Amendola, E., Zhan, Y., Mattucci, C., Castroflorio, E., Calcagno, E., Fuchs, C., Lonetti, G., Silingardi, D., Vyssotski, A.L., Farley, D. *et*

al. (2014) Mapping pathological phenotypes in a mouse model of CDKL5 disorder. *PLoS One*, **9**, e91613.

14. Okuda, K., Takao, K., Watanabe, A., Miyakawa, T., Mizuguchi, M. and Tanaka, T. (2018) Comprehensive behavioral analysis of the Cdkl5 knockout mice revealed significant enhancement in anxiety- and fear-related behaviors and impairment in both acquisition and long-term retention of spatial reference memory. *PLoS One*, **13**, e0196587.

15. Tang, S., Terzic, B., Wang, I.-T.J., Sarmiento, N., Sizov, K., Cui, Y., Takano, H., Marsh, E.D., Zhou, Z. and Coulter, D.A. (2019) Altered NMDAR signaling underlies autistic-like features in mouse models of CDKL5 deficiency disorder. *Nat. Commun.*, **10**, 2655.

16. Jhang, C.-L., Huang, T.-N., Hsueh, Y.-P. and Liao, W. (2017) Mice lacking cyclin-dependent kinase-like 5 manifest autistic and ADHD-like behaviors. *Hum. Mol. Genet.*, **26**, 3922–3934.

17. Jhang, C.-L., Lee, H.-Y., Chen, J.-C. and Liao, W. (2020) Dopaminergic loss of cyclin-dependent kinase-like 5 recapitulates methylphenidate-remediable hyperlocomotion in mouse model of CDKL5 deficiency disorder. *Hum. Mol. Genet.*, **29**, 2408–2419.

18. Adhikari, A., Buchanan, F.K.B., Fenton, T.A., Cameron, D.L., Halmai, J.A.N.M., Copping, N.A., Fink, K.D. and Silverman, J.L. (2022) Touchscreen cognitive deficits, hyperexcitability, and hyperactivity in males and females using two models of cdkl5 deficiency. *Hum. Mol. Genet.*, **00**, 1–19.

19. Strauß, M., Ulke, C., Paucke, M., Huang, J., Mauche, N., Sander, C., Stark, T. and Hegerl, U. (2018) Brain arousal regulation in adults with attention-deficit/hyperactivity disorder (ADHD). *Psychiatry Res.*, **261**, 102–108.

20. Geissler, J., Romanos, M., Hegerl, U. and Hensch, T. (2014) Hyperactivity and sensation seeking as autoregulatory attempts to stabilize brain arousal in ADHD and mania? *Atten. Defic. Hyperact. Disord.*, **6**, 159–173.

21. Martella, D., Aldunate, N., Fuentes, L.J. and Sánchez-Pérez, N. (2020) Arousal and executive alterations in attention deficit hyperactivity disorder (ADHD). *Front. Psychol.*, **11**, 1991.

22. Hebb, D.O. (1955) Drives and the C. N. S. (conceptual nervous system). Drives and the C. N. S. (conceptual nervous system). *Psychol. Rev.*, **62**, 243–254.

23. Robbins, T.W. (1997) Arousal systems and attentional processes. Arousal systems and attentional processes. *Biol. Psychol.*, **45**, 57–71.

24. Lavie, P. (1989) Ultradian rhythms in arousal–the problem of masking. *Chronobiol. Int.*, **6**, 21–28.

25. Blum, I.D., Zhu, L., Moquin, L., Kokoeva, M.V., Gratton, A., Giros, B. and Storch, K.-F. (2014) A highly tunable dopaminergic oscillator generates ultradian rhythms of behavioral arousal. *Elife*, **3**, 1–23.

26. Wainio-Theberge, S., Wolff, A. and Northoff, G. (2021) Dynamic relationships between spontaneous and evoked electrophysiological activity. *Commun. Biol.*, **4**, 1–17.

27. Park, S., Kim, D.-W., Han, C.-H. and Im, C.-H. (2021) Estimation of emotional arousal changes of a group of individuals during movie screening using steady-state visual-evoked potential. *Front. Neuroinform*, **0**, 1–10.

28. Bohlin, G. (1976) Delayed habituation of the electrodermal orienting response as a function of increased level of arousal. Delayed habituation of the electrodermal orienting response as a function of increased level of arousal. *Psychophysiology*, **13**, 345–351.

29. Sokolov, E.N. (1990) The orienting response, and future directions of its development. *Pavlov. J. Biol. Sci.*, **25**, 142–150.

30. Sokolov, E.N. (1963) Higher nervous functions; the orienting reflex. *Annu. Rev. Physiol.*, **25**, 545–580.

31. Lynn, R. (2013) Attention, Arousal and the Orientation Reaction: International Series of Monographs in Experimental Psychology. In *Attention, Arousal and the Orientation Reaction: International Series of Monographs in Experimental Psychology*. Elsevier, Amsterdam, The Netherlands.

32. Berti, S., Vossel, G. and Gamer, M. (2017) The orienting response in healthy aging: novelty P3 indicates no general decline but reduced efficacy for fast stimulation rates. *Front. Psychol.*, **8**, 1780.

33. Wang, C.-A. and Munoz, D.P. (2015) A circuit for pupil orienting responses: implications for cognitive modulation of pupil size. *Curr. Opin. Neurobiol.*, **33**, 134–140.

34. Montes-Lourido, P., Kar, M., Kumbam, I. and Sadagopan, S. (2021) Pupillometry as a reliable metric of auditory detection and discrimination across diverse stimulus paradigms in animal models. *Sci. Rep.*, **11**, 1–15.

35. Pfeffer, T., Keitel, C., Kluger, D.S., Keitel, A., Russmann, A., Thut, G., Donner, T.H. and Gross, J. (2022) Coupling of pupil- and neuronal population dynamics reveals diverse influences of arousal on cortical processing. *Elife*, **11**, 1–28.

36. Stitt, I., Zhou, Z.C., Radtke-Schuller, S. and Fröhlich, F. (2018) Arousal dependent modulation of thalamo-cortical functional interaction. *Nat. Commun.*, **9**, 2455.

37. McGinley, M.J., David, S.V. and McCormick, D.A. (2015) Cortical membrane potential signature of optimal states for sensory signal detection. *Neuron*, **87**, 179–192.

38. Storbeck, J. and Clore, G.L. (2008) Affective arousal as information: how affective arousal influences judgments, learning, and memory. *Soc. Personal. Psychol. Compass*, **2**, 1824–1843.

39. Barnard, K.E., Broman-Fulks, J.J., Michael, K.D., Webb, R.M. and Zawilinski, L.L. (2011) The effects of physiological arousal on cognitive and psychomotor performance among individuals with high and low anxiety sensitivity. *Anxiety Stress Coping*, **24**.

40. Artoni, P., Piffer, A., Vinci, V., LeBlanc, J., Nelson, C.A., Hensch, T.K. and Fagiolini, M. (2020) Deep learning of spontaneous arousal fluctuations detects early cholinergic defects across neurodevelopmental mouse models and patients. *Proc. Natl. Acad. Sci. U. S. A.*, **117**, 23298–23303.

41. Joshi, S., Li, Y., Kalwani, R.M. and Gold, J.I. (2016) Relationships between pupil diameter and neuronal activity in the locus coeruleus, colliculi, and cingulate cortex. *Neuron*, **89**, 221–234.

42. Pan, J., Klímová, M., McGuire, J.T. and Ling, S. (2022) Arousal-based pupil modulation is dictated by luminance. *Sci. Rep.*, **12**, 1390.

43. Bradley, M.M., Miccoli, L., Escrig, M.A. and Lang, P.J. (2008) The pupil as a measure of emotional arousal and autonomic activation. *Psychophysiology*, **45**, 602–607.

44. Lee, C.R. and Margolis, D.J. (2016) Pupil dynamics reflect behavioral choice and learning in a Go/NoGo tactile decision-making task in mice. pupil dynamics reflect behavioral choice and learning in a Go/NoGo tactile decision-making task in mice. *Front. Behav. Neurosci.*, **10**, 1–14.

45. Ganea, D.A., Bexter, A., Günther, M., Gardères, P.-M., Kampa, B.M. and Haiss, F. (2020) Pupillary dilations of mice performing a vibrotactile discrimination task reflect task engagement and response confidence. *Front. Behav. Neurosci.*, **14**, 159.

46. de Gee, J.W., Tsetsos, K., Schwabe, L., Urai, A.E., McCormick, D., McGinley, M.J. and Donner, T.H. (2020) Pupil-linked phasic arousal predicts a reduction of choice bias across species and decision domains. *Elife*, **9**, 1–25.

47. Mazziotti, R., Carrara, F., Viglione, A., Lupori, L., Lo Verde, L., Benedetto, A., Ricci, G., Sagona, G., Amato, G. and Pizzorusso, T. (2021) MEYE: web app for translational and real-time pupillometry. *eneuro*, **8**, 1–13.

48. Reimer, J., McGinley, M.J., Liu, Y., Rodenkirch, C., Wang, Q., McCormick, D.A. and Tolias, A.S. (2016) Pupil fluctuations track rapid changes in adrenergic and cholinergic activity in cortex. *Nat. Commun.*, **7**, 13289.

49. Wang, C.-A., Baird, T., Huang, J., Coutinho, J.D., Brien, D.C. and Munoz, D.P. (2018) Arousal effects on pupil size, heart rate, and skin conductance in an emotional face task. arousal effects on pupil size, heart rate, and skin conductance in an emotional face task. *Front. Neurol.*, **9**, 1–13.

50. Mazziotti, R., Sagona, G., Lupori, L., Martini, V. and Pizzorusso, T. (2020) 3D Printable device for automated operant conditioning in the mouse. *eNeuro*, **7**, 1–9.

51. Jones, F.N. (1939) The behavior of organisms: an experimental analysis. *Am. J. Psychol.*, **52**, 659–660.

52. Francis, N.A. and Kanold, P.O. (2017) Automated operant conditioning in the mouse home cage. *Front. Neural Circuits*, **11**, 10.

53. O'Leary, J.D., O'Leary, O.F., Cryan, J.F. and Nolan, Y.M. (2018) A low-cost touchscreen operant chamber using a Raspberry Pi™. *Behav. Res. Methods*, **50**, 2523–2530.

54. Mazziotti, R., Lupori, L., Sagona, G., Gennaro, M., Della Sala, G., Putignano, E. and Pizzorusso, T. (2017) Searching for biomarkers of CDKL5 disorder: early-onset visual impairment in CDKL5 mutant mice. *Hum. Mol. Genet.*, **26**, 2290–2298.

55. Bahi-Buisson, N., Villeneuve, N., Caietta, E., Jacquette, A., Maurey, H., Matthijs, G., Van Esch, H., Delahaye, A., Moncla, A., Milh, M. *et al.* (2012) Recurrent mutations in the CDKL5 gene: genotype-phenotype relationships. *Am. J. Med. Genet. A*, **158A**, 1612–1619.

56. Liang, J.-S., Huang, H., Wang, J.-S. and Lu, J.-F. (2019) Phenotypic manifestations between male and female children with CDKL5 mutations. *Brain Dev.*, **41**, 783–789.

57. Kluckova, D., Kolnikova, M., Medova, V., Bognar, C., Foltan, T., Svecova, L., Gnip, A., Kadasi, L., Soltysova, A. and Ficek, A. (2021) Clinical manifestation of CDKL5 deficiency disorder and identified mutations in a cohort of Slovak patients. *Epilepsy Res.*, **176**, 106699.

58. Boxhoorn, S., Bast, N., Supèr, H., Polzer, L., Cholemkery, H. and Freitag, C.M. (2020) Pupil dilation during visuospatial orienting differentiates between autism spectrum disorder and attention-deficit/hyperactivity disorder. *J. Child Psychol. Psychiatry*, **61**, 614–624.

59. Wainstein, G., Rojas-Líbano, D., Crossley, N.A., Carrasco, X., Aboitiz, F. and Ossandón, T. (2017) Pupil Size Tracks Attentional Performance In Attention-Deficit/Hyperactivity Disorder. *Sci. Rep.*, **7**, 1–9.

60. Cohen, N.J. and Douglas, V.I. (1972) Characteristics of the orienting response in hyperactive and normal children. *Psychophysiology*, **9**, 238–245.

61. Harris, N.S., Courchesne, E., Townsend, J., Carper, R.A. and Lord, C. (1999) Neuroanatomic contributions to slowed orienting of attention in children with autism. *Brain Res. Cogn. Brain Res.*, **8**, 61–71.

62. Divergent Strategies for Learning in Males and Females (2021) *Curr. Biol.*, **31**, 39–50.e4.

63. Narayanan, N.S. and Laubach, M. (2017) Inhibitory control: mapping medial frontal cortex. inhibitory control: mapping medial frontal cortex. *Curr. Biol.*, **27**, R148–R150.

64. Diamond, A. (2013) Executive functions. *Annu. Rev. Psychol.*, **64**, 135–168.

65. Schmitt, L.M., White, S.P., Cook, E.H., Sweeney, J.A. and Mosconi, M.W. (2018) Cognitive mechanisms of inhibitory control deficits in autism spectrum disorder. *J. Child Psychol. Psychiatry*, **59**, 586–595.

66. St John, T., Estes, A.M., Dager, S.R., Kostopoulos, P., Wolff, J.J., Pandey, J., Elison, J.T., Paterson, S.J., Schultz, R.T., Botteron, K. *et al.* (2016) Emerging executive functioning and motor development in infants at high and low risk for autism spectrum disorder. *Front. Psychol.*, **7**, 1016.

67. Leitner, Y. (2014) The co-occurrence of autism and attention deficit hyperactivity disorder in children - what do we know? *Front. Hum. Neurosci.*, **8**, 268.

68. Demontis, D., Walters, R.K., Martin, J., Mattheisen, M., Als, T.D., Agerbo, E., Baldursson, G., Belliveau, R., Bybjerg-Grauholm, J., Bækvad-Hansen, M. *et al.* (2019) Discovery of the first genome-wide significant risk loci for attention deficit/hyperactivity disorder. *Nat. Genet.*, **51**, 63–75.

69. Kucewicz, M.T., Dolezal, J., Kremen, V., Berry, B.M., Miller, L.R., Magee, A.L., Fabian, V. and Worrell, G.A. (2018) Pupil size reflects successful encoding and recall of memory in humans. *Sci. Rep.*, **8**, 4949.

70. Tsukahara, J.S. and Engle, R.W. (2021) Is baseline pupil size related to cognitive ability? Yes (under proper lighting conditions). *Cognition*, **211**, 104643.

71. Aston-Jones, G. and Cohen, J.D. (2005) An integrative theory of locus coeruleus-norepinephrine function: adaptive gain and optimal performance. *Annu. Rev. Neurosci.*, **28**, 403–450.

72. Neske, G.T., Nestvogel, D., Steffan, P.J. and McCormick, D.A. (2019) Distinct waking states for strong evoked responses in primary visual cortex and optimal visual detection performance. *J. Neurosci.*, **39**, 10044–10059.

73. Shimaoka, D., Harris, K.D. and Carandini, M. (2018) Effects of arousal on mouse sensory cortex depend on modality. *Cell Rep.*, **25**, 3230.

74. Woods, A.J., Philbeck, J.W. and Wirtz, P. (2013) Hyper-arousal decreases human visual thresholds. *PLoS One*, **8**, e61415.

75. Lee, T.-H., Baek, J., Lu, Z.-L. and Mather, M. (2014) How arousal modulates the visual contrast sensitivity function. *Emotion*, **14**, 978–984.

76. Rae, C.L., Hughes, L.E., Anderson, M.C. and Rowe, J.B. (2015) The prefrontal cortex achieves inhibitory control by facilitating subcortical motor pathway connectivity. *J. Neurosci.*, **35**, 786–794.

77. Zhang, S., Hu, S., Chao, H.H., Ide, J.S., Luo, X., Farr, O.M. and Li, C.-S.R. (2014) Ventromedial prefrontal cortex and the regulation of physiological arousal. Ventromedial prefrontal cortex and the regulation of physiological arousal. *Soc. Cogn. Affect. Neurosci.*, **9**, 900–908.

78. Nieuwenhuis, S., De Geus, E.J. and Aston-Jones, G. (2011) The anatomical and functional relationship between the P3 and autonomic components of the orienting response. *Psychophysiology*, **48**, 162–175.

79. Cocker, K.D., Fielder, A.R., Moseley, M.J. and Edwards, A.D. (2005) Measurements of pupillary responses to light in term and preterm infants. *Neuroophthalmology*, **29**, 95–101.

80. de Vries, L., de Vries, L., Fouquaet, I., Boets, B., Naulaers, G. and Steyaert, J. (2021) Autism spectrum disorder and pupillometry: a systematic review and meta-analysis. *Neurosci. Biobehav. Rev.*, **120**, 479–508.

81. Sekaninova, N., Mestanik, M., Mestanikova, A., Hamrakova, A. and Tonhajzerova, I. (2019) Novel approach to evaluate central autonomic regulation in attention deficit/hyperactivity disorder (ADHD). *Physiol. Res.*, **68**, 531–545.

82. Mattapallil, M.J., Wawrousek, E.F., Chan, C.-C., Zhao, H., Roychoudhury, J., Ferguson, T.A. and Caspi, R.R. (2012) The Rd8 mutation of the Crb1 gene is present in vendor lines of C57BL/6N mice and embryonic stem cells, and confounds ocular induced mutant phenotypes. *Invest. Ophthalmol. Vis. Sci.*, **53**, 2921–2927.

83. Silasi, G., Xiao, D., Vanni, M.P., Chen, A.C.N. and Murphy, T.H. (2016) Intact skull chronic windows for mesoscopic wide-field imaging in awake mice. *J. Neurosci. Methods*, **267**, 141–149.

84. Bishop, C.M. (2006) Pattern recognition and machine learning. In *Pattern Recognition and Machine Learning*. Springer, NY, USA.

85. Platt, J. (1999) Probabilistic outputs for support vector machines and comparisons to regularized likelihood methods. *Adv Large Margin Classifiers*, **10**, 61–74.

86. Rasmussen, C.E. and Williams, C.K.I. (2005) Gaussian processes for machine learning. In *Gaussian Processes for Machine Learning*. MIT Press, Cambridge, MA.

87. Hastie, T., Tibshirani, R. and Friedman, J. (2013) The elements of statistical learning: data mining, inference, and prediction. In *The Elements of Statistical Learning: Data Mining, Inference, and Prediction*. Springer Science & Business Media, NY, USA.

88. Freund, Y. and Schapire, R.E. (1997) A decision-theoretic generalization of on-line learning and an application to boosting. *J. Comput. Syst. Sci.*, **55**, 119–139.

89. Hinton, G.E. (1989) Connectionist learning procedures. *Artif. Intell.*, **40**, 185–234.